

Biochar from sugarcane bagasse for reactive dye adsorption considering a circular economy approach

Abstract

Ethanol from sugarcane has advantages over fossil fuel in reducing greenhouse gas emissions and improving the air quality in cities. However, ~280kg of sugarcane bagasse, an agro-industrial waste, are still generated during the processing of 1 ton of sugarcane. In this paper, the sugarcane bagasse, was converted into activated biochar (AB) and the physicochemical properties and morphology of the AB were determined. The potential adsorbent for reactive blue 19 dye (RB19) onto AB under different conditions was studied, considering the pH influence, adsorption isotherms, kinetic studies and thermodynamic parameters. Finally, a preliminary circular economic analysis was also performed. The characterization of AB showed microtubes of up to 1µm diameter and cavities lower than 0.5µm, with a specific surface area of 687m²/g and an iodine number of 656mg I₂/g. The Freundlich adsorption isotherm resulted in the best fit for the experimental data, with maximum adsorption of 58.1 mg/g at pH 2 and 31.4mg/g at pH 5. The adsorption took place in the first 2h, following a pseudo-second-order kinetic model. The thermodynamic experiments showed that higher temperatures improved the removal efficiency by ~10% and that the process is endothermic. The preliminary circular economic analysis for AB preparation revealed a cost of 2.18USD/Kg of adsorbent. This study indicates that AB is an economical material for large-scale wastewater treatment in textile industries, offering an alternative pathway for the agro-industrial waste generated during the ethanol production.

Keywords: textile industries, agro-industrial waste, activated biochar, adsorption of reactive dye, biomass valorization

Volume 8 Issue 4 - 2022

Fabiano Tomazini da Conceição,¹ Rodrigo Braga Moruzzi,² Guilherme Augusto Prado Duarte,¹ Lais Galileu Speranza,¹ Maria Lucia Pereira Antunes,³ Sandro Donnini Mancini³

¹Universidade Estadual Paulista (UNESP), Instituto de Geociências e Ciências Exatas, Campus de Rio Claro, Brazil

²Universidade Estadual Paulista (UNESP), Instituto de Ciência e Tecnologia, Campus de São José dos Campos, Brazil

³Universidade Estadual Paulista (UNESP), Instituto de Ciência e Tecnologia, Campus de Sorocaba, Brazil

Correspondence: Fabiano Tomazini da Conceição, Universidade Estadual Paulista (UNESP), Instituto de Geociências e Ciências Exatas, Campus de Rio Claro, Brazil, Tel +55 19 3526-9358, Email fabiano.tomazini@unesp.br

Received: August 25, 2022 | **Published:** September 08, 2022

Introduction

Aerosols from fossil fuel burning increased during the twentieth century, suggesting that they may have contributed to global temperature changes.^{1,2} On the other hand, biofuels are sources of renewable energy, which could substitute petroleum products used in several human activities.^{3,4} In particular, the ethanol from sugarcane has advantages over fossil fuel in reducing greenhouse gas emissions and improving the air quality in cities.⁵ During the 1980s, the cultivation of sugarcane for the production of ethanol in the Brazilian territory was encouraged by the federal government on the second phase of the National Alcohol Program (PROALCOOL II), generating the expansion to more than three million hectares of sugarcane plantations for ethanol production in the south-central region of Brazil.⁶

Brazil was the second-largest global producer of ethanol in 2020 (30% of the total)⁷ and the first-largest global producer of sugarcane in 2019 (39% of the total).⁸ In 2019, the volume of ethanol produced in Brazil was 10,092x10³m³, with a volume stored in January 2020 of 2,493x10³m³.⁹ The Brazilian sugarcane crops area in the 2020/2021 harvest was approximately 8.6 million hectares or 86,000km², which corresponds to an area equivalent to Austria.¹⁰ The sugarcane crops generated 654 million tons of sugarcane, converted into 41 million tons of sugar and 29 billion liters of ethanol.¹⁰ Approximately 280kg of sugarcane bagasse, an agro-industrial waste, is generated during the processing of one ton of sugarcane,¹¹ which can be burned to produce heat and electricity. The electricity generated is used in the sugar and alcohol production plants themselves and/or is sold to the electricity grid.¹² Although sugarcane bagasse burns to electricity production yields in lower emissions compared with diesel, it still releases climate change gases to the atmosphere.¹³

Consequently, the use of part of the sugarcane bagasse to produce products with greater added value and less environmental impact

could represent interesting gains for sugarcane producers in Brazil or elsewhere. One of these products can be the activated biochar, an important adsorbent commonly used for pollutants removal due to its functional groups, large superficial specific area, good chemical stability, recyclability and high mechanical strength.¹⁴ The global market for activated biochar in 2020 was 1,666x10³ton, with the water and/or wastewater treatment segment responsible for 52% of its total consumption, even considering the interest in masks with activated carbon during the COVID-19 pandemic.¹⁵ The production of activated biochar from sugarcane bagasse would fit into the circular economy concept, which has been widely promoted by government agencies, policymakers, businesses, and academia.¹⁶ It replaces the “end-of-life” definition and presents a circular process with reducing, reusing, recycling, and recovering materials during its complete life cycle (production, distribution, consumption, and disposal process).^{17,18} On green fuel production chains, such as ethanol, the application of this concept is of high importance to guarantee the sustainability of the process.⁵

The textile industries are one of the oldest and most traditional activities in the productive and profitable segments of the world. They are responsible for an important part of the Brazilian and world economy.¹⁹ However, they are characterized by high water consumption and the generation of large volumes of liquid effluents that can be toxic and causes several environmental problems.^{20,21} For the removal of color from textile effluents, the most known and studied processes are coagulation/flocculation, adsorption, and oxidative processes.²² However, adsorption is the technique that presents the best results and the one that has the greatest application in removing the color of textile effluents.²³ One of the most common dyes used by the textile industry is the reactive blue 19 (RB19). Some studies presented the feasibility of the biochar for RB19 removal, such as grapefruit peel,²⁴ dried pulp and paper sludge,²⁵ citrus waste,²⁶ coconut shell,^{27,28} pomegranate seed powder,²⁹ rice straw ash³⁰ and pistachio shell.³¹

Although there are several studies involving the RB19 removal by different activated biochar, no studies were carried out using activated biochar produced with sugarcane bagasse (AB). Therefore, this study aims to assess the RB19 removal from an aqueous solution onto AB. The physicochemical properties and morphology of the AB were determined. The effects of the pH, the adsorption isotherms models, the kinetics study, and the thermodynamic parameters were also investigated. Finally, a preliminary economic analysis was also carried out to understand the opportunities in the circular economy related to the sugar cane bagasse, an important agro-industrial waste, which can be used as a low-cost adsorbent on cleaner production in textile industries in Brazil and elsewhere.

Materials and methods

Activation and characterization of the activated biochar

The activated biochar (AB) with ZnCl (20mol/L), in the proportion of 1:3 (g:mL), was produced with sugarcane bagasse via pyrolysis at 600°C and 1h residence time under nitrogen gas atmosphere.³² After activation, the material was washed with distilled water for 30min, and the mixture was centrifuged at 350rpm for 20min. Then, the AB was separated and dried in an oven at 60°C for 24h. The pH value for AB was characterized using the ratio 1:25 (g of AB per mL of distilled and deionized water), with an equipment trademark YSI, model 556. Patterns of high purity were used for calibration of pH 4.00 (4.00±0.01 at 25°C±0.2°C) and 7.00 (7.00±0.01 at 25°C±0.2 °C).

The specific surface area (SSA) was measured by BET/N₂ adsorption, using a Micromeritics ASAP 2010 instrument. According to the Brazilian Association of Technical Standards (EB-2133-ABNT, 1991), the iodine number was measured (in mg I₂/g of AB), which determined the adsorption characteristics of AB. The infrared spectrum of AB was determined by ATR FT-IR (Varian), with a wavelength range from 400-4000cm⁻¹. Finally, the morphology of AB was identified using a Scanning Electron Microscope (SEM, JEOL JSM-6010LA).

Removal experiments

The reactive blue 19 dye (RB19), an anionic azo-dye, whose characteristics are shown in Table 1, was used in this study. All batch adsorption experiments were carried out in triplicate. The RB19 aqueous solutions (V=50mL) were mixed with AB (m=0.2g). The RB19 concentrations were measured using a Hach DR-2800 spectrophotometer at a wavelength of 590nm,³³ and deionized water was used as control. The amount of RB19 adsorbed onto the AB at equilibrium time, q_e (mg/g), and the adsorption percentage (%A) were determined using equations 1 and 2, respectively.^{34,35}

$$q_e = \frac{C_0 - C_e}{m} \cdot V \quad (1)$$

$$\%A = \frac{C_0 - C_e}{C_0} \cdot 100 \quad (2)$$

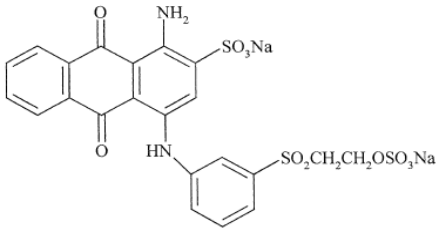
Where: C_0 and C_e are the initial and equilibrium concentrations of RB19, respectively (mg/mL), m is the mass of AB (g), and V is the volume of solution (mL).

The pH influence and adsorption studies

According to the pH range, the solubility of dyes can be reduced or increased. Thus, the pH influence on the adsorption of RB 19

into the AB adsorbent was carried out with C_0 of 300mg/L at 25°C and in different pH values (2, 3, 5, 7, 9, and 12). The samples were stirred for 6 h at 120 rpm and the pH control was made with HCl and NaOH, 0.1 M. As presented in item 3.2 (Influence of pH on the RB19 removal), the best pH for RB19 removal was 2. As achieving pH 2 at a commercial scale is challenging, pH 5 was also tested on further studies. Therefore, the effect of initial concentration, the adsorption and kinetics studies and the temperature influence were assessed at pH 2 and 5.

Table 1 Main characteristics of the Reactive Blue 19 dye (RB19)

Molecular structure	
Generic name	C.I. Reactive Blue 19
Molecular formula	C ₂₂ H ₁₆ N ₂ O ₁₁ S ₃ Na ₂
Molar mass	626.54g/mol
Class	Reactive
λ _{máx} (nm)	590
1000	22

For adsorption experiments, different initial concentrations (C_0) were investigated, i.e., 50, 150, 200, 300, 400, 500, 800, and 1000mg/L, based on the two selected pH values of 2 and 5 at 25°C, with the samples stirred at 120rpm for 6h. After this period, in both experiments carried out, the solutions were centrifuged for 20min at 3500rpm, and the remaining concentration (C_e) of RB19 in the supernatant was measured. The Freundlich (Equation 3) and Langmuir (Equation 4) adsorption isotherms were applied for adsorption modelling.²²

$$q_e = k_F C_e^{1/n} \quad (3)$$

$$q_e = \frac{q_{max} k_L C_e}{1 + k_L C_e} \quad (4)$$

Where: k_F is the Freundlich capacity factor [(mg/g)/(mL/mg)^{1/n}], $1/n$ is the Freundlich intensity parameter, q_{max} is the maximum amount of adsorption corresponding to complete monolayer coverage on the surface (mg/g), and k_L is the Langmuir constant related to the energy of adsorption (mL/mg).

Adsorption kinetics

The kinetics studies were carried out in C_0 of 300 mg/L for pH 2 and 5 at 25°C. The suspensions were stirred at 120 rpm and sampled at 15, 30, 60, 120, and 420 min and the C_e of RB19 was determined as described above. The pseudo-first-order Lagergren (Equation 5) and pseudo-second-order (Equation 6) models were applied to determine kinetics constants and explain the reaction mechanisms.³⁵

$$\frac{dq_t}{dt} = k_1 (q_e - q_t) \quad (5)$$

$$\frac{dq_t}{dt} = k_2 (q_e - q_t)^2 \quad (6)$$

Where: q_t and q_e are the amount adsorbed at equilibrium (mg/g) and at any time t (min), respectively, k_1 and k_2 are the rate constant of

pseudo-first-order rate (1/min) and pseudo-second-order adsorption (g/mg/min), respectively.

The temperature influence on the adsorption

The temperature influence on adsorption of RB19 at different temperatures, i.e., 303 K (30°C), 313 K (40°C), and 323 K (50°C) was studied using C_0 of 300mg/L, at pH 2 and 5, with the C_e of RB19 measured as described previously. The standard free energy or Gibbs energy (ΔG° -J/mg) was obtained from equations 7 and 8, and the enthalpy change (ΔH° -J/mg) and the entropy (ΔS° -J/mg/K) were determined from the slope and intercept of the linear trendline of the van't Hoff equation (Equation 9).

$$\Delta G^\circ = -R.T. \ln K_c \quad (7)$$

$$k_c = \frac{C_0}{C_e} \quad (8)$$

$$\ln k_c = -\frac{\Delta H^\circ}{R.T} + \frac{\Delta S^\circ}{R} \quad (9)$$

Where: R is the gas constant (J/mol/K), k_c is the adsorption equilibrium constant, T is the temperature (K), $-\Delta H^\circ/R$ is the slope of the van't Hoff chart, and $\Delta S^\circ/R$ is the intercept of the van't Hoff chart.

Average relative error

The average relative error (ARE–Equation 10) and R^2 were conjointly used in both isotherm and kinetics investigations in order to evaluate the best data fit to models.³⁶ ARE results were also used to evaluate models under (+) and over (-) prediction.

$$ARE (\%) = \frac{100}{N} \left(\frac{|exp| - |cal|}{|exp|} \right) \quad (10)$$

Where: $|exp|$ and $|cal|$ are the experimental and calculated values, respectively, for either isotherm or kinetic investigations, N = sample size.

Results and discussion

Characterization of AB

The AB possesses a pH value of 9.8 and SSA of 687m²/g. The pH value of 9.8 is higher than the pH_{PCZ} (6.4).³² indicating negative charges on AB surface. In Brazil, the values higher than 600mgI₂/g for the iodine number indicates if the activated biochar can be used in the water treatment plants – WTP (EB-2133-ABNT 1991). The iodine number for the AB was 656mgI₂/g, suggesting the use of the AB in Brazilian WTP. The AB was analyzed by SEM to characterize its surface morphology (Figure 1a). The AB is composed of fragments of different sizes, shapes and textures since the AB is a heterogeneous material with microtubes varying from 0.6 to 1.0µm in diameter and several cavities and pores lower than 0.5µm. The high porosity helps the dye to be trapped and adsorbed by the AB.³⁷

The FT-IR spectrum shows peaks at 3389, 1587, 1377, 1221, 1098 and 797cm⁻¹ (Figure 1b), which represent several functional groups. The broad peak detected at 3389 cm⁻¹ is due to O–H stretching vibrations of hydroxyl functional groups, such as phenolic or aliphatic alcohol and carboxylic acid.^{38–40} The peak at 1587cm⁻¹ is related to aromatic ring models (C=C stretching), while the peaks at 1377, 1221 and 1098cm⁻¹ represent the C–H bending (–CH₃), amine (C–N) and C–O of a primary alcohol, respectively.³⁷ Finally, the peak at 797cm⁻¹ is due to the =C–H in alkenes.³⁹

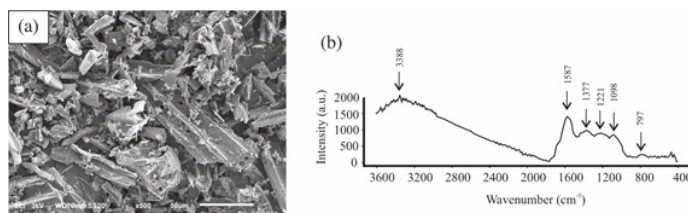


Figure 1 Scanning electron microscopy (SEM) images of AB (a). FT-IR spectrum of AB (b).

Influence of the pH on the RB19 removal

The analysis of RB19 removal demonstrated a different percentage of removal for pH 2 and 5 (Table 2), with relative standard deviations lower than 3%. The pH 5 presented RB19 adsorption percentages varying from 12 to 56%, as a function of the initial concentration (C_0). The pH 2 presented the highest adsorption percentage of RB19, with values between 22 and 68%. Additionally, the highest RB19 removals at pH 2 and 5 were obtained for lower initial concentrations, while for the elevated initial concentrations, the removal in both pH values decreased to 22 and 12%, respectively. Thus, the results show clearly that the initial RB19 concentration plays a significant role in the RB19 adsorption process by AB.

Table 2 Adsorption percentage (%A) of RB19 onto the AB, at pH 2 and 5

C_0 (mg/L)	pH2	pH5
50	68	56
100	54	53
200	50	35
300	43	28
400	42	25
500	24	22
800	25	15
1000	22	12

The pH_{PCZ} is another important issue on RB19 removal by AB, once it determines whether electrostatic attraction or repulsion between the sorbents and sorbates. At the pH values used in the experimental procedures (2 and 5), the AB in solutions with pH values lower than the pH_{PCZ} (6.4).³² developed a positive charge on their surface, resulting in the electrostatic attraction that exists between the positively charged surface of the AB and the anionic RB19. The acid pH values (lower than 3) were suggested to maximum removal of RB19 using different adsorbents.^{24–26,28–31}

Adsorption isotherms

The Freundlich (Equation 3) and Langmuir (Equation 4) adsorption isotherms at different pH values are presented in Figure 2. The parameters of both models are shown in Table 3. The highest values of R^2 and the lower ARE values were obtained using the Freundlich model for both pH values studied. However, the R^2 values and the maximum adsorption capacity suggest that the Langmuir model is also adequate. The Freundlich model considers the non-uniformity of real surfaces and describes the ionic adsorption within certain limits of concentration. Freundlich adsorption isotherm was considered as the better isotherm model in other studies reported in the literature (Table 4).

The maximum adsorption was 58.1mg/g at pH 2 and 31.4 mg/g at pH 5. The highest k_f value was obtained for pH 2, confirming its highest adsorption capacity in relation to pH 5. Table 4 also displays the comparison of AB adsorption capacity of this study with other

studies elsewhere. The maximum adsorption of 58.1mg/g at pH 2 was higher than the other studies involving different AB, even in more acidic environments, highlighting the advantage of the use of sugarcane bagasse as an adsorbent of RB19 in relation to other AB.

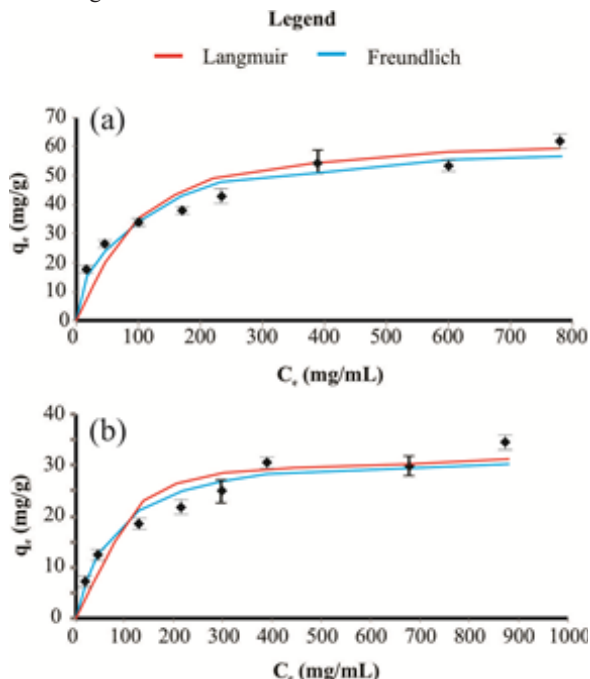


Figure 2 Adsorption isotherms of RB19 by AB at pH 2 (a) and 5(b), using Langmuir and Freundlich adsorption models. Bars indicate standard deviation.

Table 3 Parameter of adsorption using Freundlich and Langmuir models for RB19 adsorption by AB, at pH 2 and 5

pH	Freundlich parameter			Langmuir parameter				
	kF [(mL/mg) ^{1/n}]	1/n	R ²	ARE (%)	q _{max} (mg/g)	kL (mL/mg)	R ²	ARE (%)
2	2.57	0.49	0.99	6.7	58.1	0.006	0.99	9.1
5	2.27	0.38	0.99	7.3	31.4	0.012	0.99	10.2

Table 4 Comparison of AB adsorption capacity (q_{max} in mg/g) with other studies at ~ 25°C

Adsorbent	pH	q _{max}	Reference
Sugar cane bagasse	2	58.1	Present study
Grapefruit peel	3	12.4	²⁴
Dried pulp and paper sludge	3	4.1	²⁵
Citrus waste	--	14.8	²⁶
Coconut shell	12	2.2	²⁷
Coconut shell	2	57	²⁸
Pomegranate seed powder	3	3.6	²⁹
Rice straw fly ash	1	38.2	³⁰
Pistachio shell	2	2.2	³¹

Kinetic studies

Figure 3 and Table 5 show the adsorption kinetics of RB19 by AB at pH 2 and 5. It demonstrates that the adsorption reactions are typical biphasic kinetics, with fast RB19 adsorption happening in the first 2h, and a further increase in time does not improve the adsorption capacity. Therefore, the reaction does not need to be extended to a longer time. Using the maximum adsorption of 58.1mg/g at pH 2 and 31.4mg/g at pH 5 and 120min as the adsorption limit time, transfer rate of 0.48 and 0.26mg/g/min, can be obtained for the RB19 adsorption on AB at pH 2 and 5, respectively.

The kinetic parameters presented in Table 5 were obtained from the adjustment of the kinetic models to the experimental adsorption data, at pH 2 and 5, using pseudo-first-order Lagergren and pseudo-second-order. Comparing the q_t versus adsorption time of RB19 by AB at pH 2 and 5 (Figure 3) for pseudo-first-order Lagergren and pseudo-second-order kinetic models and their adjustment to the experimental data based on the ARE values and R² (Table 5), the adsorption kinetics fits better with the pseudo-second-order kinetic model. The pseudo-second-order was also the best kinetic model in the studies of activated biochar from grapefruit peel,²⁴ coconut shell,^{27,28} pomegranate seed powder,²⁹ rice straw fly ash³⁰ and pistachio shell.³¹

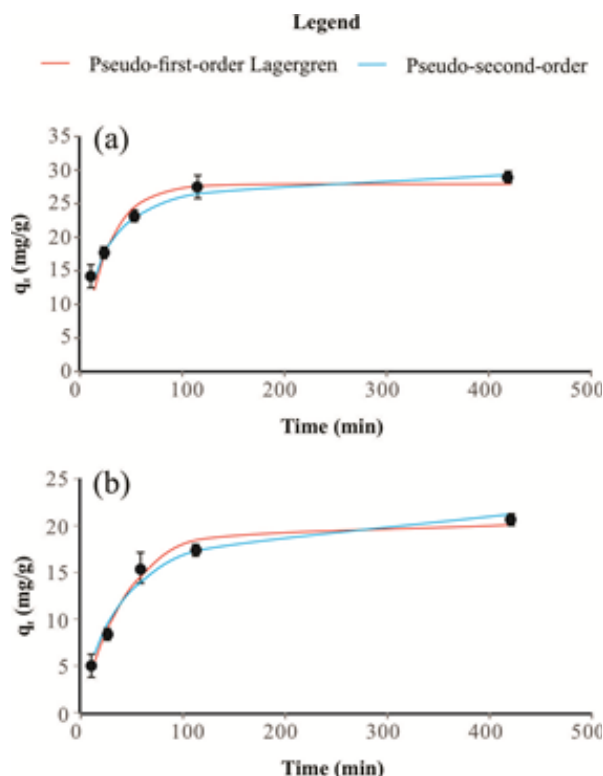


Figure 3 q_t versus adsorption time of RB19 by AB at pH 2 (a) and 5 (b) adjusted by pseudo-first order Lagergren and pseudo-second-order. Bars indicate standard deviation.

Table 5 Kinetic parameters obtained by pseudo-first-order and pseudo-second-order models for RB19 adsorption by AB, at pH 2 and 5

Kinetic parameter	pH	
	2	5
Pseudo-first-order		
q _e (mg/g)	27.68	z
k ₁ (1/min)	0.04	0.02
R ²	0.95	0.98
ARE	6.2	5.6
Pseudo-second-order		
q _e (mg/g)	30.48	23.06
k ₂ × 10 ³ (g/mg/min)	1.79	1.09
R ²	0.97	0.99
ARE	4.8	5.1

Thermodynamic studies

The thermodynamic studies indicated an increase in the percentage of adsorption of RB19 by AB of ~10% with increasing temperatures (Figure 4a), ranging from 42-53% for pH 2 and 28-38% to pH 5. Thermodynamic parameters of enthalpy, entropy and Gibbs energy (at 303, 313 and 323 K) were calculated at pH 2 and 5 and are presented

in Table 6. The constants ΔH° and ΔS° were obtained from the slope and intercept of plot $\ln k_c$ versus $T^{-1} \cdot 10^3$ (van't Hoff chart) (Figure 4b), respectively. Positive values for ΔH° (4.21 and 8.22 kJ/mg for pH 2 and 5, respectively) suggested an endothermic process, while positive ΔS° (average of 0.05J/mg/K) indicated affinity of the AB for RB19.⁴² For ΔG° , negative values were observed, confirming the natural spontaneity of the adsorption process. The decrease of ΔG° with increasing temperature suggests an increase in adsorption affinity of RB19 for AB with temperature.^{41,42}

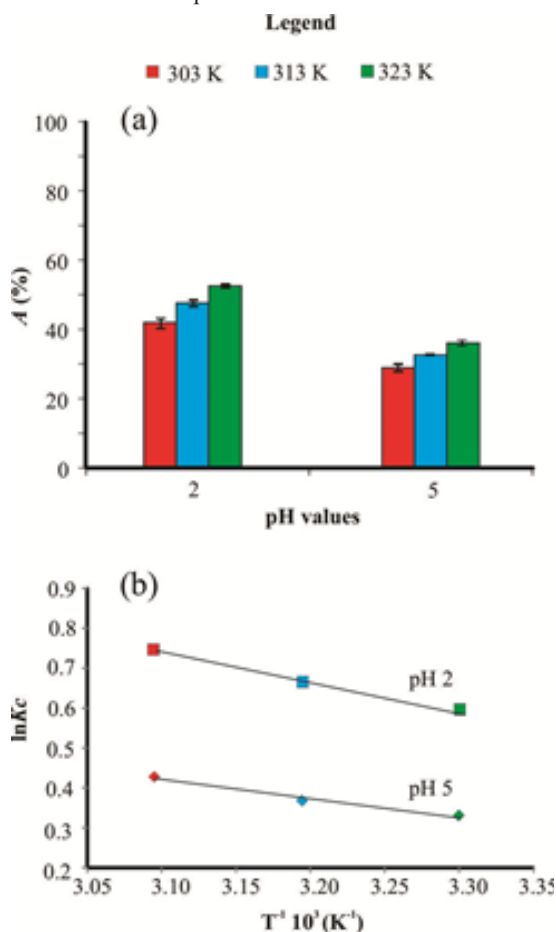


Figure 4 Adsorption of RB19 by AB at different temperatures (a) and van't Hoff chart (b). Bars indicate standard deviation.

Table 6 Kinetic parameters obtained by pseudo-first-order and pseudo-second-order models for RB19 adsorption by AB, at pH 2 and 5

pH	ΔH° (kJ/mg)	ΔS° (J/mg/K)	ΔG° (kJ/mg)		
			303 (K)	313 (K)	323 (K)
2	4.21	0.02	-1.36	-1.68	-1.99
5	8.22	0.03	-0.86	-0.99	-1.2

Implications for circular economy

Finally, a preliminary economic analysis was also carried out to understand the opportunities in the circular economy related to the sugarcane bagasse and its real field application in wastewater treatment from textile industries. The overall cost of AB preparation includes the chemical and energy costs. The main use of the sugarcane bagasse in the production of heat and electricity in thermoelectric plants. Based on the sugarcane bagasse burning in a thermoelectric plant in the Paraíba State (Brazil), indicated that ~1.4kg of sugarcane bagasse is necessary to generate 1kWh of electricity.¹³ In Brazil, the average cost for generating electricity is US\$ 0.10 per kWh,⁴³ which yields US\$

0.10 to the mill owner. Considering the Brazilian market price for 1kg of AB (US\$ 9.50) and that 1 kg of sugarcane bagasse generates 230g of AB, a cost of US\$ 2.18 per ABkg can be calculated. Consequently, a minimum added value up to 31-fold can be obtained in relation to the sugarcane bagasse burning to generate electricity. The last harvest generated 654 million tons of sugarcane,¹⁰ corresponding to 182 million tons of sugarcane bagasse, used to generate electricity. If part of this total amount of sugarcane bagasse were converted into AB, the circular economy would be applied. This agro-industrial waste would be applied not only for the generation of electricity but also a product with high added value, with excellent adsorbent properties for the removal of reactive dye during the wastewater treatment from textile effluents.

Conclusion

Ethanol produced from sugarcane crops helps to reduce the main aerosols related to the greenhouse effect. However, during ethanol production, a large amount of sugarcane bagasse is generated. Here, we produced the activated biochar from sugarcane bagasse and studied its potential adsorbent for the removal of reactive blue 19 dye (RB19) from an aqueous solution. The highest removal value was achieved at pH 2 (68%) for the lower initial concentrations. The maximum achieved adsorption capacity was 58.1mg/g at pH 2 and 31.4 mg/g at pH 5, with an initial concentration of 300mg/g at 25°C. The Freundlich adsorption isotherm was the better adjustment for the experimental data. The adsorption reactions happen in the first 2h, obeying a pseudo-second-order kinetic model, based on the chemical adsorption. The thermodynamic studies indicated an endothermic process and affinity of AB for RB19. The results obtained in this study showed clearly that the AB has higher adsorption capacity and fast adsorption kinetics than other studies involving different activated biochar elsewhere. In addition, a preliminary circular economic analysis indicated a low cost for AB preparation, with an added value up to 31-fold in relation to the sugarcane bagasse burning to generate electricity. Therefore, the use of sugarcane bagasse would not have its useful life ended during the generation of electricity but prolonged due to extremely useful product obtained, which could be used as a low-cost material highly efficient adsorbent in wastewater treatment from textile industries.

Acknowledgments

The authors acknowledge the Fundação de Amparo à Pesquisa do Estado de São Paulo (FAPESP - Processes No. 2009/02374-0 and 2013/00994-6) and the Conselho Nacional de Desenvolvimento Científico e Tecnológico (CNPq - Process No. 480555/2009-5). In addition, Guilherme Duarte is grateful to Conselho Nacional de Desenvolvimento Científico e Tecnológico (CNPq) for the scholarship (Processes No. 36991/2016 and 43110/2017).

Funding

None.

Conflicts of interest

The authors declare no conflicts of interest regarding the publication of this manuscript.

References

- Novakov T, Ramanathan V, Hansen JE, et al. Large historical changes of fossil-fuel black carbon aerosols. *Geophysical Research Letters*. 2003;30(6).

2. Ito A, Penner JE. Historical emissions of carbonaceous aerosols from biomass and fossil fuel burning for the period 1870–2000. *Global Biogeochemical Cycles*. 2005;19:GB2028.
3. Martinelli LA, Filoso S. Expansion of sugarcane ethanol production in Brazil: environmental and social challenges. *Ecol Appl*. 2008;18(4):885–898.
4. Hira A, Oliveira LGO. No substitute for oil? How Brazil developed its ethanol industry. *Energy Policy*. 2009;37(6):2450–2456.
5. Goldemberg J, Coelho ST, Guardabassi P. The sustainability of ethanol production from sugarcane. *Energy Policy*. 2008;37(6):2450–2456.
6. Adami M, Rudorff BFT, Freitas RM, et al. Remote sensing time series to evaluate direct land use change of recent expanded sugarcane crop in Brazil. *Sustainability*. 2012;4(4):574–585.
7. USDE – United States Department of Energy. Global ethanol production by country or region, 2020. 2021.
8. FAO – Food and Agriculture Organization of United Nations. Statistical Yearbook 2021. 2022.
9. Brazil – National agency of petroleum, natural gas and biofuels. Production of Biofuels. 2020.
10. CONAB – Companhia Nacional de Abastecimento (Brazilian Supply Agency). Monitoring the Brazilian sugarcane crop. 2022.
11. Karp SG, Woiciechowski AL, Soccol VT, et al. Pretreatment strategies for delignification of sugarcane bagasse: a review. *Brazilian Archives of Biology and Technology*. 2013;56:679–689.
12. Rípoli TCC, Molina Júnior WF, Rípoli MLC. Energy potential of sugarcane biomass in Brazil. *Scientia Agricola*. 2000;57(4):677–681.
13. Carvalho M, Segundo VBS, Medeiros MG, et al. Carbon footprint of the generation of bioelectricity from sugarcane bagasse in a sugar and ethanol industry. *International Journal of Global Warming*. 2019;17:235–251.
14. Wang X, Cheng H, Ye G, et al. Key factors and primary modification methods of activated carbon and their application in adsorption of carbon-based gases: A review. *Chemosphere*. 2022;287(Pt 2):131995.
15. MORDOR – Mordor Intelligence: Activated Carbon Market. Growth, Trends, Covid–19 Impact, and Forecasts (2021–2026). 2020.
16. Korhonen J, Honkasalo A, Seppälä J. Circular Economy: The Concept and its Limitations. *Ecological Economics*. 2018;143:37–46.
17. Geissdoefer M, Savaget P, Bocken NMP, et al. The Circular Economy – A new sustainability paradigm? *Journal of Cleaner Production*. 2017;143:757–768.
18. Kirchherr J, Reike D, Hekkert M. Conceptualizing the circular economy: An analysis of 114 definitions. *Resources, Conservation and Recycling*. 2017;127:221–232.
19. Batista PCS, Lisboa JVO, Augusto MG, et al. Effectiveness of business strategies in Brazilian textile industry. *Revista Administração*. 2016;51:225–239.
20. Blackburn R. Sustainable textiles: life cycle and environmental impact. Woodhead Publishing; 2009.
21. Yek PNY, Peng W, Wong CC, et al. Engineered biochar via microwave CO₂ and steam pyrolysis to treat carcinogenic Congo red dye. *J Hazard Mater*. 2020;395:122636.
22. Tchobanoglous G, Burton FL, Stensel HD. Wastewater engineering: Treatment and reuse. 4th edn. Metcalf & Eddy, Inc; 2003.
23. Gök Ö, Özcan SS, Özcan A. Adsorption behavior of a textile dye of Reactive Blue 19 from aqueous solutions onto modified bentonite. *Applied Surface Science*. 2010;256:5439–5443.
24. Abassi M, Asl NR. Removal of hazardous reactive blue 19 dye from aqueous solutions by agricultural waste. *J Iran Chem Res*. 2009;2:221–230.
25. Azizi A, Moghaddam MR, Arami M. Application of wood waste for removal of reactive blue 19 from aqueous solution; optimization through response surface methodology. *Environmental Engineering Management Journal*. 2012;11:795–804.
26. Asgher M, Bhatti HN. Evaluation of thermodynamics and effect of chemical treatments on sorption potential of Citrus waste biomass for removal of anionic dyes from aqueous solutions. *Ecological Engineering*. 2012;38:79–85.
27. Isah UA, Abdullaheem G, Bala S, ET AL. Kinetics, equilibrium and thermodynamics studies of C.I. Reactive Blue 19 dye adsorption on coconut shell based activated carbon. *International Biodeterioration & Biodegradation*, 2015;102:265–273.
28. Muralikrishnan R, Jodhi C. Biodecolorization of reactive dyes using biochar derived from coconut shell: batch, isotherm, kinetic and desorption studies. *Chemistry Select*. 2020;5:7734–7742.
29. Dehviri M, Ghaneian MT, Ebrahimi A, et al. Removal of reactive blue 19 dyes from textile wastewater by pomegranate seed powder: isotherm and kinetic studies. *International Journal of Environmental Health Engineering*. 2016;5:5.
30. El-Bindary AA, Abd El-Kawi MA, Hafez AM, et al. Removal of reactive blue 19 from aqueous solution using rice straw fly ash. *J Mater Environ Sci*. 2016;7:1023–1036.
31. Rahdar S, Shikhe L, Ahmadi S. Removal of Reactive Blue 19 dye using a combined sonochemical and modified pistachio shell adsorption processes from aqueous solutions. *Iranian Journal of Health Sciences*. 2018;6:8–20.
32. Seixas FL, Gimenes ML, Fernandes-Machado NRC. Treatment of vinasse by adsorption on sugarcane bagasse charcoal. *Química Nova*. 2016;39:172–179.
33. Souza KC, Antunes MLP, Couperthwaite SJ, et al. Adsorption of reactive dye on seawater-neutralized bauxite refinery residue. *Journal of Colloid and Interface Science*. 2013;396:210–214.
34. Conceição FT, Pichinelli BC, Silva MSG, et al. Cu(II) adsorption from aqueous solution using red mud activated by chemical and thermal treatment. *Environmental Earth Sciences*. 2016;75:36.
35. Conceição FT, Silva MSG, Menegário AA, et al. Precipitation as the main mechanism for Cd(II), Pb(II) and Zn(II) removal from aqueous solution using natural and activated forms of red mud. *Environmental Advances*. 2021;4:100056.
36. Pichinelli BC, Silva MSG, Conceição FT, et al. Adsorption of Ni(II), Pb(II) and Zn(II) on Ca(NO₃)₂-neutralized red mud. *Water, Air and Soil Pollution*. 2017;228:24.
37. Mahmoodi NM, Hayati B, Arami M, et al. Adsorption of textile dyes on Pine Cone from colored wastewater: Kinetic, equilibrium and thermodynamics studies. *Desalination*. 2011;268:117–125.
38. Lam SS, Liew RK, Lim XY, et al. Fruit waste as feedstock for recovery by pyrolysis technique. *International Biodeterioration & Biodegradation*. 2016;113:325–333.
39. Mahmoud ME, Nabil GM, El-Mallah NM, et al. Kinetics, isotherm, ad thermodynamic studies of the adsorption of reactive red 195 A dye from water by modified Switchgrass Biochar adsorbent. *Journal of Industrial and Engineering Chemistry*. 2016;37:156–167.
40. Liew RK, Nam WL, Chong MY, et al. Oil palm waste: An abundant and promising feedstock for microwave pyrolysis conversion into good quality biochar with potential multi-applications. *Process Safety and Environmental Protection*. 2018;115:57–69.

41. Aksakal O, Uzun H. Equilibrium, kinetic and thermodynamic studies of the biosorption of textile dye (Reactive red 195) onto *Pinus silvestris* L. *Journal of Hazardous Materials*. 2010;181:666–672.
42. Chowdhury S, Mishra R, Saha P, et al. Adsorption thermodynamics, kinetics and isosteric heat of adsorption of malachite green onto chemically modified rice husk. *Desalination*. 2011;265:159–168.
43. ANEEL – Agência Nacional de Energia Elétrica (Brazilian Agency of Electricity). Ranking de tarifas (Price ranking). 2022.